Deexcitation of Fast He, Ne, and Ar Metastable Atoms in Various Gases*

John T. Moseley, J. R. Peterson, D. C. Lorents, and M. Hollstein†
Stanford Research Institute, Menlo Park, California 94025
(Received 13 March 1972)

Absolute cross sections for the deexcitation of $He(2\,^1S)$ and of $He(2\,^3S)$ metastables by N_2 and Ar have been measured over the energy interval from 150 to 1600 eV using an optical technique. The $2\,^1S$ cross sections are found to be as much as 50% larger than the $2\,^3S$ cross sections for deexcitation by N_2, while for Ar the two cross sections are nearly equal at these energies. The cross sections all lie in the range of 7–20 Å^2 and decrease with increasing energy. Deexcitation cross sections have also been measured by collecting slow ions for mixed beams of He metastables in N_2, Ar, and C_2H_2 and for mixed beams of Ar metastables in C_2H_2 and Ne metastables in Ar. These measurements are in the energy range from 50 to 600 eV. They do not discriminate between different metastable states, but the results exhibit an energy behavior similar to that of the state-separated measurements and are consistent with those measurements when comparison can be made.

INTRODUCTION

Interactions between metastable, electronically excited atoms (or molecules) and ground-state species are of interest both for the basic understanding of energy-transfer mechanisms and for their importance in the upper atmosphere, in lasers, and in other excited-gas media. There have been several investigations at thermal energies,[1-3] but few at higher energies because of the difficulty in producing and detecting the metastables. Some effective deexcitation cross sections have been deduced for $He(2\,^3S)$ at energies above 10 keV from beam equilibrium studies,[4] $H(2S)$ has been studied using electric quenching techniques,[5,6] and the excitation transfer of $He(2\,^1S$ and $2\,^3S)$ in He and of $N_2(A\,^3\Sigma_u^+)$ in N_2 and NO has been studied in this laboratory[7,8] at incident energies between about 150 and 2200 eV. The importance of metastables and their interactions for atmospheric processes is discussed in a review by Dalgarno.[9]

We report here on measurements of absolute cross sections for the deexcitation of $He(2\,^1S)$ and of $He(2\,^3S)$ in collisions with N_2 and Ar at incident energies between 150 and 1600 eV, using an optical method[7] to discriminate between the $2\,^1S$ and $2\,^3S$ components in a mixed beam. We also present the results of some earlier measurements,[10] in which the deexcitation of metastable beams by various gases was studied by measuring the spatial decay of slow ions produced in the gas. Since for each target gas studied here, the ionization potential of the target is less than the excitation energy of the metastable, such slow ions are produced by Penning ionization. These "slow-ion" measurements do not distinguish between different metastable states in a mixed beam. They were used to study He^* deexcitation in N_2, Ar, and C_2H_2; Ar^* in C_2H_2; and Ne^* in Ar. The He^*+N_2 and He^*+Ar results from the two measurements are consistent. The He^*+Ar and Ne^*+Ar results are compared with recent theoretical calculations by Olson.[11,12]

OPTICAL MEASUREMENTS

Method

A well-collimated, neutral He beam, containing both $He(2\,^1S)$ and $He(2\,^3S)$ atoms, as well as some ground-state $He(1\,^1S)$ atoms, with well-defined velocities, is prepared by neutralization of a He^+ beam by charge-transfer collisions in an alkali vapor.[7] Absolute deexcitation cross sections are obtained separately for $He(2\,^1S)$ and $He(2\,^3S)$ by observing the spatial decay of each excited component of the beam as the beam passes through a gas at known pressures. The singlet and triplet components can be monitored separately, as the following argument shows. Most inelastic collisions between the He^* and the target-gas particles deexcite the He^* by ionizing the target (Penning ionization), a process that is the major fraction of the measured deexcitation cross sections. However, in a very small fraction of the collisions, the He^* atoms are further excited to higher states. Radiations from $n=3$ states are observed in this experiment. The He^* excitation cross sections are much smaller than the deexcitation cross sections, but they are much larger than those that would excite the same levels from He^0 (ground-state) collisions at these velocities[13]; thus the He^0 component of the beam is not observed, and the He I emissions may be used to monitor the metastable component. Furthermore, spin conservation in the collision dictates that, for instance, $He(2\,^1S)$ atoms can only be excited to higher singlet states unless the N_2 (or Ar) target (in a singlet state) is simultaneously excited to a triplet state.

Such double excitations are at least 6 (or 11) eV more endothermic than the single He excitations and are negligible at these beam energies. A similar spin conservation rule also applies to the He($2\,^3S$) atoms. We also find (see below) no evidence of cascading from $4F$ or similar higher levels of mixed spins.[14] Thus by observing photons from an appropriate singlet or triplet transition, the $2\,^1S$ and $2\,^3S$ components can be monitored independently in a mixed beam. By measuring the attenuation of their intensity as a function of target-gas pressure and beam path length, absolute cross sections are obtained without knowledge of the beam composition.

Interference filters were used to isolate the singlet line at 6678 Å ($3\,^1D \rightarrow 2\,^1P$) and the triplet lines at 7065 Å ($3\,^3P \rightarrow 2\,^3P$) and 5876 Å ($3\,^3D \rightarrow 2\,^3P$). The 3889-Å line ($3\,^3P \rightarrow 2\,^3S$) was also used in the Ar measurements, but contributions from the 3914-Å N_2^+ first negative band precludes its state selectivity for He*-N_2 collisions. Earlier studies[13] of the spectra produced by He* in various gases assured that the lines used were free from other interference.

Apparatus

A schematic of the apparatus is given in Fig. 1. He^+ ions are produced in a hot-filament dc discharge by electrons with a maximum energy of 80 eV. The ions are accelerated to the desired energy, mass selected, and directed into a charge-transfer oven containing potassium vapor at a pressure of about 10^{-4} Torr. Atoms in the $2\,^1S$ and $2\,^3S$ states of He are formed by near-resonant charge transfer of the He^+ ions with potassium. The remaining ions are deflected from the beam immediately on exiting the oven, and the mixed beam of singlet and triplet He metastables, along with some ground-state He, continues into the collision chamber. In this chamber, the deexciting gas is maintained at a known constant pressure in the range 1 to 50×10^{-4} Torr.

Two identical front surface mirrors, oriented at 45° and 135° to the beam direction (see Fig. 1), sample light from the metastable beam at two positions separated by 15 cm. Centered between these mirrors is a third, larger mirror that can be rotated to direct the light from either sampling mirror vertically through a quartz lens and a quartz window in the vacuum wall, through an optical interference filter, and onto the cathode of a Freon-cooled photomultiplier tube.

The cross section Q can be calculated from the ratio of the photon counting rates from the two beam segments I_1/I_2 by the relation[7]

$$Q = (1/nd)\,[\ln(I_1/I_2) - \ln\alpha] \;, \tag{1}$$

where n is the gas number density, and d is the distance between observation points. The quantity α is the ratio of the light collection efficiencies for the two light paths, and it was determined experimentally by two techniques. From Eq. (1), I_1/I_2 approaches α as n approaches zero. Operation of the collision chamber at pressures less than 2×10^{-5} Torr yielded negligible beam deexcitation, but sufficient signal to allow a determination of $\alpha = (I_1/I_2)_{p=0}$. A second and more accurate technique is to obtain data at fixed energy, but over a wide range of pressures, and require that α have a value such that Q in Eq. (1) remains constant. Determinations by both techniques were in agreement. Although α changed whenever physical changes were made along the light paths, its value was always near 1.

The pressure in the collision chamber was measured using a capacitance manometer (MKS Baratron) and maintained constant to within 1% by a servocontrolled leak valve. The capacitance manometer was calibrated by the manufacturer just before the measurements described here, and this calibration was further checked during the measurements using a McLeod gauge. Symmetric trapping of the gauge system was employed to eliminate errors due to thermal transpiration, and He was used as a test gas to reduce possible errors due to mercury vapor streaming (Gaede effect) to less than 2%. The total uncertainty in the pressure measurement is ±4%.

SLOW-ION MEASUREMENTS

The slow-ion measurements were conducted in the apparatus of Fig. 1 except for the interaction region. The deactivation cell used for the slow-ion measurements is shown in Fig. 2. This method, which is also an attenuation measurement, is applicable in cases where slow ions are produced in abundance by the excited beam, such as in Penning ionization collisions. A module containing three identical cylindrical ionization cavities was constructed in which the slow ions produced in three equal segments of the beam path were collected. Two additional end cavities isolated the three inner cavities from any end effects. The cavities were electrically isolated from each other by double grids that spanned the 2-in. apertures, each with a transparency of 99%. The ions were collected on two wire rings that are maintained at ground potential in each of the cavities. The cavities were held at +65 V, thus creating a potential well for the ions inside the cavities. At these potentials, the collected current was fully saturated. The small surface area of the rings reduced the possible photoelectron current to negligible levels. Operational amplifiers mounted in the vacuum chambers were used to amplify the ion currents before measurement. The outputs of

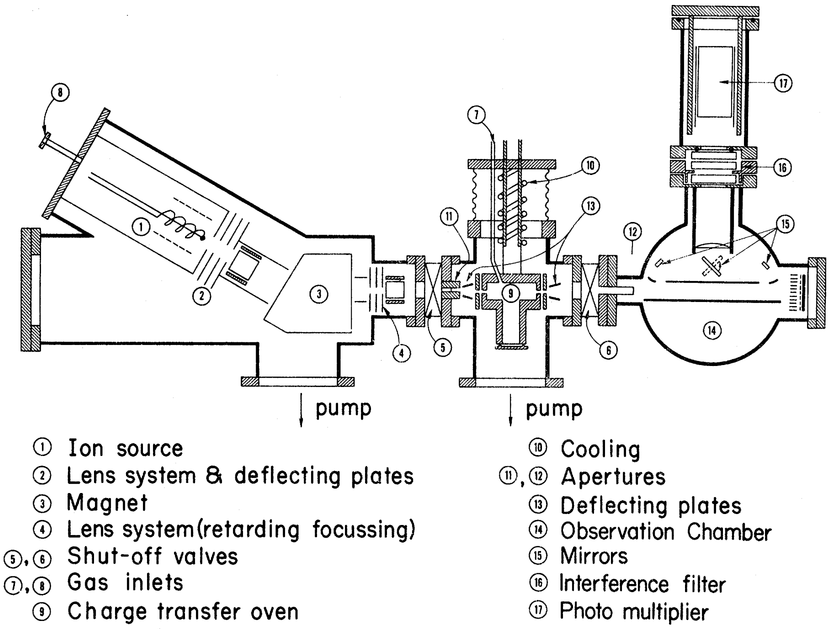

FIG. 1. Schematic of the apparatus as used for the state-selected measurements.

the three op-amps were scanned in less than 0.5 sec using a Vidar data-acquisition system that digitized and stored the data on magnetic tape. At least 30 scans were averaged at each pressure. This procedure was repeated for 6 to 10 different pressures, which produced total attenuations in the 5–50% range. The cross sections obtained from these data were independent of pressure except at the low-pressure end where an unexplained 5–10% increase occurred. The pressure independent values were averaged for the results reported here.

We assume that ionization caused by ground-state atoms in the beam is negligible. This is justified because the ground-state ionization cross sections are less than 10^{-16} cm^2 in the energy range of the measurements while the observed cross sections are greater than 10^{-15} cm^2.

Under these conditions the ratio of two different cavity currents is given by

$$I_1/I_2 = I_2/I_3 = e^{nQl} , \tag{2}$$

$$I_1/I_3 = e^{2nQl} , \tag{3}$$

where l is the length of each cavity. At any point in the interaction region, the state-unselected cross sections Q are related to the state-selected cross sections by the equation

$$Q = f_1 Q_1 + f_3 Q_3 , \tag{4}$$

where f_1 and f_3 are the singlet and triplet fractions of the metastable component of the beam at the point in question. The initial values of f_1 and f_3 are determined by the charge-transfer reaction and thus depend upon the beam energy and the charge-transfer vapor used, but if $Q_1 \neq Q_3$, f_1 and f_3 will also change as the beam passes through the target gas, and will depend on the difference in the cross sections, the gas pressure, and the distance traveled through the gas. For these measurements it can be shown that (for a given beam energy) f_1 and f_3 usually varied by less than 5% over the interaction path. Thus, the measured cross sections are represented by the average given by Eq. (4), where f_1 and f_3 are the initial singlet and triplet fractions.

Aside from the uncertainties in the scattering corrections discussed below, the errors in the slow-ion measurements are estimated to be less than ± 10%, including systematic errors introduced by the pressure dependences and errors in the pressure, length, and current measurements.

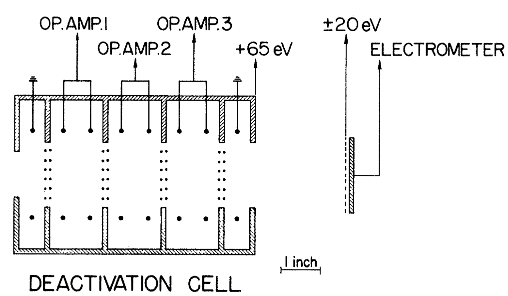

FIG. 2. Deactivation cell used for the slow-ion measurements.

EFFECTS OF SCATTERING

The attenuation of the metastable component of the beams is mainly due to excitation transfer, but some loss also occurs through angular scattering out of the beam. To a good approximation the total attenuation cross sections obtained from the data represent the sum of the energy-transfer (deexcitation) cross section and an effective cross section for scattering out of the last detection region, suitably averaged over the path including the first detection region.

The scattering contribution is most significant at low-beam energies and for light projectiles and heavy target particles. To estimate the contribution of $He^* + Ar$ scattering to the attenuation cross section, we have used the known $He^+ + Ar$ total differential scattering cross sections that are based on a detailed analysis of experimental data taken over a wide range of energies.[15] Since the scattering contribution in this case comes mainly from fairly large scattering angles involving small impact parameters, the $He^* + Ar$ interaction is well represented by the $He^+ + Ar$ interaction. Furthermore, there will be no significant difference in the scattering of the two metastable states.

The total cross section for scattering at angles $\theta \geq \theta_i$ was obtained by integration of the reduced differential cross sections $\rho = \theta \sin\theta\sigma(\theta)$ from curve 3 of Fig. 2 in Ref. 15; thus

$$Q(\tau_1) = 2\pi \int_{\tau_1}^{\infty} \frac{\rho(\tau)}{\tau}\, d\tau \ ,$$

where $\tau_1 = E\theta_1$, and $Q(\tau_1)$ is a single curve representing the total scattering cross sections for scattering through reduced angles $\tau \geq \tau_1$, and can be used to derive the effective cross section at any energy. These cross sections were appropriately integrated and averaged over the beam paths, using the actual apparatus geometry to obtain effective scattering cross sections as a function of beam energy for both the slow-ion and optical measurements. These contributions were subtracted from the measured total cross sections to yield the pure deexcitation cross sections which are discussed below. The corrections varied from about 20% at 70 eV to about 5% at 600 eV for the slow-ion data, and from about 22% at 200 eV to about 10% at 1500 eV in the optical case. The corrections are probably accurate to 30%, and thus add about 6% uncertainty to the cross sections. The corrections greatly improved the agreement between the slow-ion data and the optical results. The slow-ion data, which include smaller scattering contributions, lay below the optical data in uncorrected form.

No scattering data exist for $He^* + N_2$ in the τ range of importance here, but after considering the small-angle data of Amdur, Mason, and Jordan[16] plus a comparison between $He^+ + Ar$ and $He^+ + Ne$,[15] as well as data for $Li^+ + N_2$ and $Li^+ + O_2$,[17] it was concluded that in the τ range of importance here (10^3-10^5 eV deg) an effective cross section two-thirds of the value obtained for $He^* + Ar$ would be accurate to at least 40% for $He^* + N_2$. The correction amounts to less than 10% of the measured total cross sections; thus the precision of the correction is adequate.

For $He^* + C_2H_2$, the angular-scattering contribution should be very similar to that for $He^* + N_2$, and since the correction is relatively small, the $He^* + N_2$ cross sections were used. The corrections were less than 7% of the total values.

Because of the large mass of Ar^*, the scattering effects were regarded as negligible in the $Ar^* + C_2H_2$ case which has the largest total cross section.

For $Ne^* + Ar$, a repulsive potential was constructed using values for $Na^+ + Ar$ calculated by Menendez *et al.*,[18] which could be closely represented in a screened Coulomb form $V(r) = (a/r) \times e^{-r/b}$ in the region of importance (r in the range 0.5–2.5 a.u.). Differential scattering cross sections, over a suitable range of angles and energies, were then calculated by Olsen,[19] using this potential. Finally, these differential cross sections were integrated and suitably averaged to account for scattering along the path in the slow-ion measurements. The $Ne + Ar$ scattering should be slightly smaller than $Na^+ + Ar$, but not significantly for τ values of importance here. The computed total cross sections agree quite well (within 20%) with Ne and Ar results of Amdur and Mason, and we estimate their over-all accuracy at ± 50%. The resulting corrections range from about 25% of the total cross section at 120 eV to 14% at 600 eV, and have been applied to the original data to yield the $Ne^* + Ar$ deactivation cross sections discussed below.

RESULTS

$He^* + N_2$

The cross sections for the deexcitation of He $(2\,^1S)$ and $(2\,^3S)$ atoms in N_2 are shown in Fig. 3. The closed triangles represent the $2\,^1S$ measurements made by observing the $3\,^1D \rightarrow 2\,^1P$ transition (6678 Å); the closed circles are the $2\,^3S$ measurements using the $3\,^3D \rightarrow 2\,^3P$ transition (5876 Å). The open squares represent the state-unselected slow-ion measurements. The error bars on the state-selected measurements include the statistical uncertainty in the data and the uncertainty in the correction for angular scattering. In addition, there is a possible systematic error of ± 6% result-

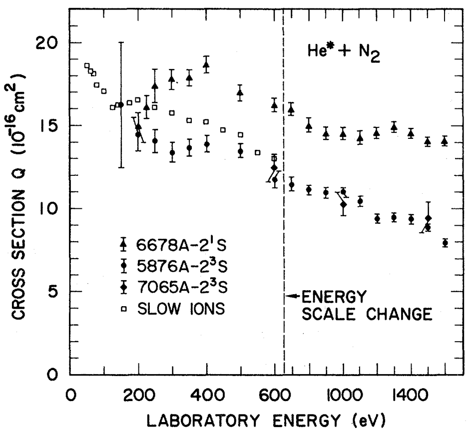

FIG. 3. He* + N_2 results.

ing from uncertainties in the pressure and path-length measurements, and in the determination of α. The total probable error in the slow-ion measurements is $\pm 15\%$.

If the $3\,^1D$ and the $3\,^3D$ levels are populated significantly by cascading from $4F$ or similar higher levels of mixed spins,[14] the assumption that the observed $3\,^1D \rightarrow 2\,^1P$ and $3\,^3D \rightarrow 2\,^3P$ transitions are representative of the singlet and triplet cross sections, respectively, is weakened. In fact, if these levels were entirely populated through such cascading, and if the singlet-triplet mixing is complete, the observed cross sections would be identical. Clearly this extreme is not the case. In an attempt to determine if cascading is significant, observations were made on the $3\,^3S \rightarrow 2\,^3P$ transition (7065 Å), because it is very unlikely that $4F$ or higher levels contribute significantly to the population of the $3\,^3S$ level. These data are represented by the closed diamonds in Fig. 3. If the $3\,^3D \rightarrow 2\,^3P$ data are affected by cascading, it would be expected that they would yield larger cross sections than the $3\,^3S \rightarrow 2\,^3P$ data. It can be seen from Fig. 3 that this is not the case; both observations are in agreement. It is concluded that cascade effects are not likely to be significant in these measurements.

It was not feasible to use the $3\,^3S \rightarrow 2\,^3P$ transition for the majority of the measurements because its low intensity made it difficult to obtain data below 600 eV. The $3\,^3P \rightarrow 2\,^3S$ transition (3889 Å) could not be used because of interference from the N_2^+ first negative band at 3914 Å.

According to Eq. (4), the cross sections from the slow-ion measurements should lie between the $2\,^1S$ and $2\,^3S$ cross sections Q_1 and Q_3. Except for the region around 200 eV, where the errors in Q_1 and Q_3 are large, this is seen to be the case. In principle, it is possible to determine the relative population of singlets and triplets in the mixed beam using three measurements such as these. However, in the $He^* + N_2$ case (which is a favorable one since the $2\,^1S$ and $2\,^3S$ cross sections are reasonably separated) cross-section measurements with an accuracy of about 1% would be required to determine the relative population with an accuracy of about 10%.

The $He^* + N_2$ cross sections decrease with increasing energy. However, the singlet cross section appears to have a maximum near 300 eV and to decrease toward lower energy, whereas the triplet cross section continues to rise. Although the statistical errors are somewhat large due to weak signals at these low energies, this decrease appears to be real. Both cross sections are expected to decrease at low energies[11,12] (below 10 eV), but neither the location nor the abruptness of the observed decrease is understood at present. Some structure is observed in both the singlet and triplet cross sections, and it seems probable that this maximum is a part of that structure.

$He^* + Ar$

The $He^* + Ar$ results are given in Fig. 4. In these results, the singlet and triplet cross sections (triangles and circles, respectively) are nearly equal over the observed energy range, and the unselected measurements (squares) are well within the combined possible errors. For the triplet cross sections, the $3\,^3P \rightarrow 2\,^3S$ transition (3889 Å) was observed. This line should be less subject to cascading than the $3\,^3D \rightarrow 2\,^3P$ transition used for the $He^* + N_2$ measurements, and it is unlikely that the similarity of the singlet and triplet data is due to cascade effects. In the following paper,[11] Olson presents calculations using realistic model potentials for both the singlet and triplet Penning ionization cross sections and compares them with these results. These calculations lie slightly below the results presented here, but have a similar energy dependence. The difference in

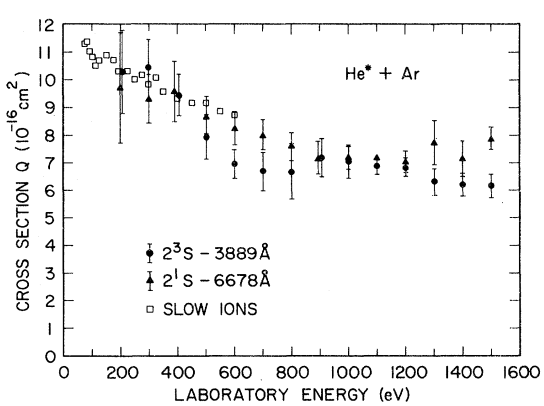

FIG. 4. He* + Ar results.

magnitude may be the result of small contributions from other deactivation processes.

He* + He

A few measurements were also made on the $He(2\,^3S)+He$ deactivation cross section (symmetric energy transfer) as a check on earlier measurements[8] made in this laboratory. The earlier measurements had a possible systematic error of ± 25% primarily because of uncertainty in the pressure determination. The new measurements yielded cross sections in good agreement with the earlier work, and it is now possible to reduce the uncertainty caused by systematic error in the earlier work to ± 10%.

Slow-Ion Measurements

The state-unselected cross sections for $He^*+C_2H_2$ are presented in Fig. 5, along with the He^*+N_2 and He^*+Ar results. All these cross sections exhibit similar energy dependencies, decreasing with increasing energy. Figure 6 shows state-unselected Ne^*+Ar cross sections measured at energies above 80 eV and compares them with a calculation by Olson[12] of the cross section for Penning ionization. In these calculations, a Morse potential was used and the coupling width was adjusted so that the low-energy data of Tang *et al.*[2] were best reproduced in the 0.01–0.1-eV range. The calculated curve lies about 15% below our experimental results and exhibits the same energy dependence.

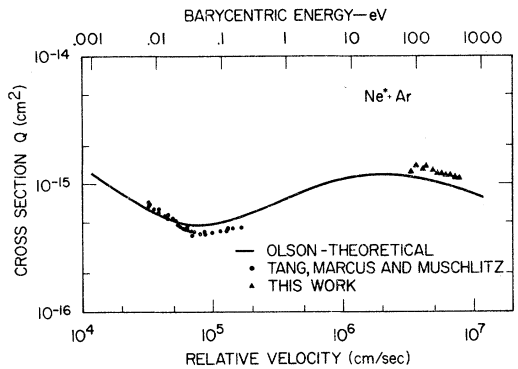

FIG. 6. Ne^*+Ar measurements compared with theory.

DISCUSSION

The cross sections reported here include all processes (except angular scattering, which has been accounted for) that remove the metastable atoms from the beam. In all of these collision partners the excitation energy of the metastable atom exceeds the ionization potential of the target. Thus, the initial state of the collision complex is imbedded in a continuum and is subject to rapid autoionization. This process (Penning ionization) is expected to be the predominant mode of deexcitation under these conditions. Metastables may also be removed by collisional ionization (i.e., $He^*+X \rightarrow He^+ + e + X$), but these processes are about 4 eV endothermic for rare-gas metastables and require a much closer encounter than do the Penning reactions, and in any case are at least partially accounted for in the angular-scattering corrections, which include all elastic and inelastic angular scattering. Removal by excitation to higher states that can radiate to the ground state can be similarly discounted except possibly for the $2\,^1S \rightarrow 2\,^1P$ transition in He, which is only 0.5 eV endothermic and may contribute a small amount to the $He(2\,^1S)$ deexcitation cross sections. $He(2\,^3S)$ atoms excited to the $2\,^3P$ state rapidly decay back to the $2\,^3S$ state and are not lost.

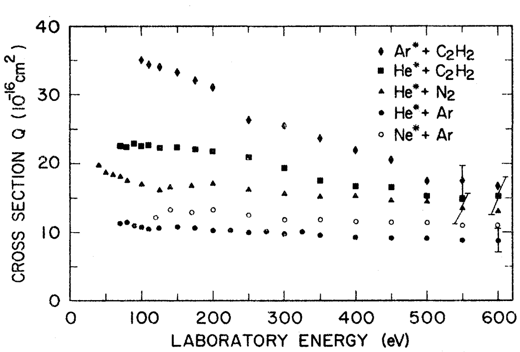

FIG. 5. Slow-ion-measurements results.

We thus associate these cross sections primarily with Penning ionization reactions, and, to our knowledge, they are the first to be measured at nonthermal energies. The fact that, where comparisons can be made, the cross sections for these exothermic reactions are larger than those at thermal energies is of interest. Unlike the He^*+He symmetric energy-transfer reactions,[7] which are inhibited at thermal energies by a small repulsive potential barrier, Olson's analysis in the adjoining paper[11] indicates that these Penning cross sections have a maximum at higher energies, because the coupling to the continuum state becomes much stronger at the smaller internuclear separations that are reached.

ACKNOWLEDGMENTS

We wish to express our appreciation to Jack Harvey of Lawrence Radiation Laboratory, Berkeley for his assistance and the use of his facilities in the calibration check of the capacitance manometer and to George Conklin and Ralph Leon for their assistance in construction and maintenance of the apparatus.

*Work supported in part by the Office of Naval Research and in part by the Advanced Research Projects Agency through the Army Research Office (Durham).

†Present address: Dornier GmbH, Friedrichshafen (Bodensee), West Germany.

[1] A. L. Schmeltekopf and F. C. Fehsenfeld, J. Chem. Phys. 53, 3173 (1970), and references listed in this paper.

[2] S. Y. Tang, A. B. Marcus, and E. E. Muschlitz, J. Chem. Phys. 56 , 566 (1972).

[3] H. Hotop and A. Niehaus, Chem. Phys. Letters 8, 497 (1971).

[4] R. E. Miers, A. S. Schlachter, and L. W. Anderson, Phys. Rev. 183, 213 (1969).

[5] H. B. Gilbody, R. Browning, R. M. Reynolds, and G. I. Riddell, *Seventh International Conference on the Physics of Electron and Atomic Collisions, Amsterdam, The Netherlands*, 1971, *Abstracts of Papers* (North-Holland, Amsterdam, 1971), p. 1080. Also G. Spiess, A. Valance, and P. Pradel, *ibid.*, p. 1083.

[6] F. W. Byron, R. V. Krotkov, and J. A. Madeiros, Phys. Rev. Letters 24, 83 (1970).

[7] M. Hollstein, J. R. Sheridan, J. R. Peterson, and D. C. Lorents, Phys. Rev. 187, 118 (1969).

[8] J. R. Sheridan and J. R. Peterson, J. Chem. Phys. 51, 3574 (1969).

[9] A. Dalgarno, Ann. Geophys. 26, 601 (1970).

[10] M. Hollstein, D. C. Lorents, and J. R. Peterson, Bull. Am. Phys. Soc. 13, 197 (1968).

[11] R. E. Olson, following paper, Phys. Rev. 6, 1031 (1972).

[12] R. E. Olson, Chem. Phys. Letters 13, 307 (1972).

[13] M. Hollstein, A. Salop, J. R. Peterson, and D. C. Lorents, Phys. Letters 32A, 327 (1970).

[14] C. C. Lin and R. G. Fowler, Ann. Phys. (N.Y.) 15, 461 (1961).

[15] F. T. Smith, R. P. Marchi, W. Aberth, D. C. Lorents, and O. Heinz, Phys. Rev. 161, 31 (1967).

[16] I. Amdur, E. A. Mason, and J. E. Jordan, J. Chem. Phys. 27, 527 (1957).

[17] W. Aberth and D. C. Lorents, Phys. Rev. 182, 162 (1969).

[18] M. G. Menendez, M. J. Redmon, and J. F. Aebischer, Phys. Rev. 180, 69 (1969).

[19] R. E. Olson (private communication).

PHYSICAL REVIEW A VOLUME 6, NUMBER 3 SEPTEMBER 1972

Semiempirical Calculations of the He* (2^3S and 2^1S) + Ar Ionization Total Cross Sections*

Ronald E. Olson

Stanford Research Institute, Menlo Park, California 94025

(Received 13 March 1972)

The ionization (associative and Penning) total cross sections for He*(2^3S) + Ar and He*($2\,^1S$) + Ar have been calculated from 10^{-3} to 10^4 eV and compared with experimental data. The classical calculations used interaction potentials that agreed with *ab initio* theoretical calculations for the repulsive wall, possessed the correct long-range energy dependence, and were in agreement with glory-scattering experiments. The coupling width was an exponential with its free parameter determined by the thermal-energy ionization cross section for each system. The calculations were then extended over a wide range of energies. It was found that as the collision energy increased at the very low energies, the cross sections decreased until about 0.1 eV where they began slowly to rise. As the collision energy is further increased, the cross sections reach a maximum of about 15 Å^2 around 10 eV, and then decrease again at higher energies. The cross sections predicted by the high-energy results, 100–1500 eV, are compared with the data of Moseley, Peterson, Lorents, and Hollstein (preceding paper) and are found to agree within 20% and to have a similar energy dependence.

INTRODUCTION

The energy dependence of the ionization (associative and Penning) total cross sections for Ne*($2p^5 3s\,^3P$) + Ar were first reported by Micha, Tang, and Muschlitz.[1] These cross sections stimulated interest to try to understand the unexpected energy dependence that was observed.[1,2] In the energy range investigated, the measured cross sections were found first to decrease with increasing energy, then to pass through a minimum around 0.05 eV, and finally to rise gently at the higher energies ($E \gtrsim 0.05$ eV). In a previous paper,[2] this author was able to explain this phenomenon and theoretically reproduce these low-energy data by using available potential curves for the Ne* + Ar interaction and a realistic exponential form for the coupling to the continuum. Basically, this behavior occurs because of the exponentially increasing nature of the coupling width as the distance of closest approach decreases with increasing energy. Furthermore, these calculations led to the prediction that the cross sections would rise to a maximum of about 10 Å^2 at around 10 eV and then slowly decrease with increasing energy. There were, however, at that time no high-energy